Green Chemistry

PAPER

View Article Online
View Journal | View Issue

Cite this: *Green Chem.*, 2019, **21**, 5039

Developing a sustainable route to environmentally relevant metal–organic frameworks: ultra-rapid synthesis of MFM-300(Al) using microwave heating†

Ieuan Thomas-Hillman, [a] Lee A. Stevens,[a] Marcus Lange,[b] Jens Möllmer,[b] William Lewis, [c,d] Chris Dodds, [a] Samuel W. Kingman [a] and Andrea Laybourn *[a]

Received 11th July 2019,
Accepted 1st August 2019

DOI: 10.1039/c9gc02375e

rsc.li/greenchem

NO_2, SO_2 and CO_2 are major air pollutants causing significant environmental and health problems. Metal–organic frameworks (MOFs), in particular $[Al_2(OH)_2(C_{16}O_8H_6)](H_2O)_6$ (trivial names: NOTT-300/MFM-300(Al)), have shown great promise for capturing these gases. However MOF syntheses often involve toxic solvents and long durations which are inherently energy intensive, an environmental burden, and have serious safety risks. There is a pressing need to develop environmentally-friendly routes to MOFs that require less energy and implement safer solvents particularly when considering scale-up beyond the laboratory for industrial application. We report the rapid synthesis of MFM-300(Al) in aqueous conditions and 10 minutes using microwave heating. This is the fastest reported synthesis of MFM-300(Al) to date with a 99.77% reduction in reaction time compared to the current reported 3-day conventionally heated route. The microwave synthesized sub-micron crystalline material exhibits gas uptake capacities of 8.8 mmol g^{-1} at 273 K and 1.0 bar for CO_2, 8.5 mmol g^{-1} at 298 K and 0.17 bar for SO_2, and 1.9 mmol g^{-1} at 298 K and 0.01 bar for NO_2. These are 26%, 70%, and 90% greater for CO_2, SO_2, and NO_2, respectively, when compared to previously reported MFM-300(Al) materials produced *via* a 3-day conventionally heated route demonstrating the production of high quality materials in a fraction of the time with enhanced gas properties. Crucially, this offers an opportunity to move from batch to continuous processing owing to reduced reaction times underpinned by targeted heating.

The dioxides of nitrogen, sulfur and carbon (NO_2, SO_2 and CO_2, respectively) are regarded as three of the most problematic air pollutants generated by anthropogenic activity.[1–3] NO_2 and SO_2 are particularly detrimental to the environment[3–5] and human health[1,6,7] as they contribute to toxic photochemical smog and acid rain.[8] Additionally, the escalating level of atmospheric CO_2 is a major environmental concern due to its implication in global warming.[3,9] The harmful effects of NO_2, SO_2 and CO_2 have provided significant impetus for their removal and the development of a sustainable low-carbon economy.

Metal–organic frameworks (MOFs) are subset of co-ordination polymers that show great potential for gas storage and separation owing to their exceptionally high surface areas and tuneable pore environment and functionalities.[8,9] Notably $[Al_2(OH)_2(C_{16}O_8H_6)](H_2O)_6$ (trivial names: NOTT-300/MFM-300(Al)) has shown exceptional selective reversible adsorption and uptake capacity of CO_2, SO_2, low-concentration NO_2 (5000 to <1 ppm), and ammonia.[10–17] A highly sensitive SO_2 sensor based on the indium analogue of MFM-300 was also recently reported.[18] However, current methods of preparing MFM-300 and indeed many other MOFs, hinders their adoption in industrial gas storage and separation applications.[19] MOFs are commonly synthesised *via* solvothermal batch reactions which involve large volumes of toxic solvent and long reaction times (up to one week).[20] The development of routes that reduce the product cost and environmental burden of MOFs is critical for the transfer of these materials from the laboratory to industry and the realisation of the environmental benefits that these materials offer.[21] In order to address these synthetic challenges, electrochemical, sonochemical, mechanochemical, spray drying, continuous flow, and microwave methods have been developed.[20,22] Of these routes, microwave heating has

[a]*Faculty of Engineering, University of Nottingham, Nottingham, NG7 2RD, UK. E-mail: Andrea.Laybourn@nottingham.ac.uk*
[b]*Institut für Nichtklassische Chemie e.V., Permoserstrasse 15, 04318 Leipzig, Germany*
[c]*School of Chemistry, University of Nottingham, Nottingham NG7 2RD, UK*
[d]*School of Chemistry, The University of Sydney, New South Wales 2006, Australia*
† Electronic supplementary information (ESI) available: Further synthetic details. See DOI: 10.1039/c9gc02375e

been shown to offer highly significant benefits such as exceptionally rapid reactions (on the order of seconds),[23] control over particle morphology and size, and phase selectivity.[21]

In this paper we describe an aqueous microwave-assisted method for synthesising MFM-300(Al) on the tens of milligrams scale in 10 minutes. This is the first time a microwave route to MFM-300(Al) has been reported. This route requires significantly less time than the current procedure (3-day solvothermal synthesis at 210 °C)[12] and negates the requirement for a corrosive piperazine additive,[12] whilst delivering MFM-300(Al) at a higher percentage yield (83 *cf.* 75%) with a highly uniform particle size and morphology and significantly enhanced uptake capacities for CO_2, SO_2 and NO_2.

A 4 : 1 mixture of aluminium chloride hexahydrate and biphenyl-3,3′,5,5′-tetracarboxylic acid (H_4BPTC) in deionized water was heated, with stirring, at 210 °C in a commercial CEM Discover microwave cavity for 10 minutes. Further synthetic details, including method development, are given in the Experimental section. Note: Temperature was determined by an in-built infra-red sensor and therefore represents the average temperature of the reaction mixture. The resulting suspended particles of microwave synthesised MFM-300(Al) (hereby denoted MFM-300(Al)-MW) were found to be 249–790 nm long and between 74–964 nm wide, with a stubby cylindrical to cuboidal morphology (Fig. 1). This differs from the plate-like sub-micron particles previously reported for MFM-300(Al)[12] prepared using conventional heating (hereby denoted MFM-300(Al)-CH) and is a likely consequence of the different heating mechanism promoting a different mode of crystal growth.[21,23] Reflections in the powder X-ray diffraction (PXRD) pattern of MFM-300(Al)-MW were indexed to the $I4_122$ tetragonal space group, corresponding to the reported crystal structure of MFM-300(Al)-CH (Fig. 2).[12] A simulated Le Bail fit[24] to the $I4_122$ space group revealed the presence of a low intensity extra reflection at around 27° 2θ (Fig. 2) attributed to residual unreacted linker (H_4BPTC). However, there was no detectable evidence of unreacted linker by thermogravimetric analysis, *i.e.* no loss at the decomposition temperature of H_4BPTC (340 °C) was observed (Fig. 3). No peaks corresponding to γ-Al(O)OH[25] or other MOF phases beyond MFM-300(Al) were observed. Attempts to synthesise MFM-300(Al) using these conditions with conventional heating for 24 to 72 hours (rather than rapidly using microwaves) gave a mixture of MOF phases and γ-Al(O)OH.[25]

Low pressure CO_2 adsorption–desorption isotherms of MFM-300(Al)-MW at ambient temperatures (273–303 K,

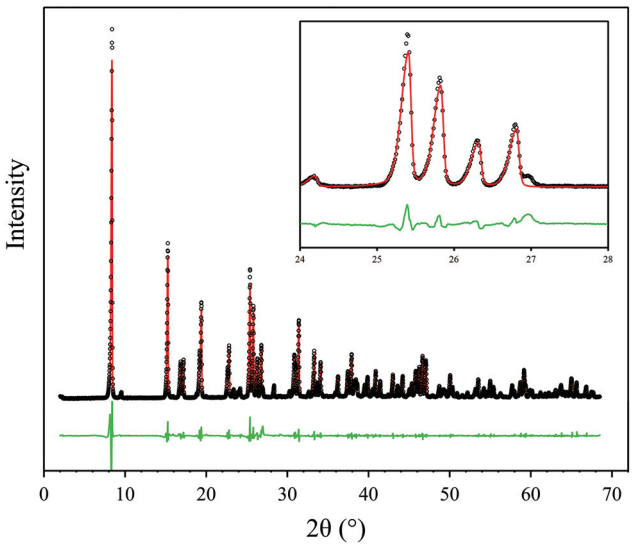

Fig. 2 PXRD pattern of MFM-300(Al)-MW. Black = observed; red = simulated pattern Le Bail fit; green = difference plot. Inset: Plot of the PXRD pattern between 24 and 28° 2θ; an extra reflection attributed to unreacted linker is visible at ~27° 2θ in the difference plot.

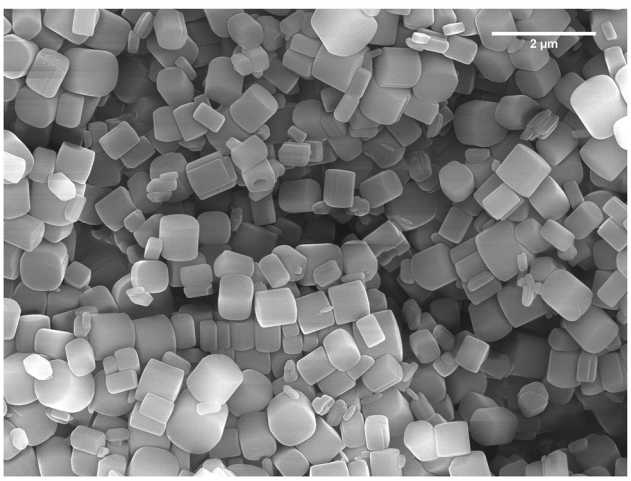

Fig. 1 SEM image of MFM-300(Al)-MW synthesised in deionized water in 10 minutes. The material exhibits average particle dimensions of 604 ± 111 × 520 ± 234 nm.

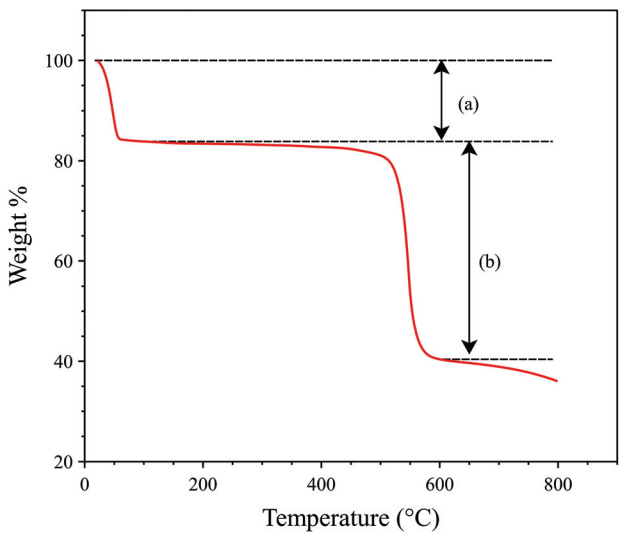

Fig. 3 TGA thermogram of MFM-300(Al)-MW. (a) 30–100 °C = loss of adsorbed water (15.85%) from the MOF. (b) 465–600 °C = thermal decomposition of MFM-300(Al)-MW (40.23%). Slow MOF decomposition is observed beyond 600 °C.

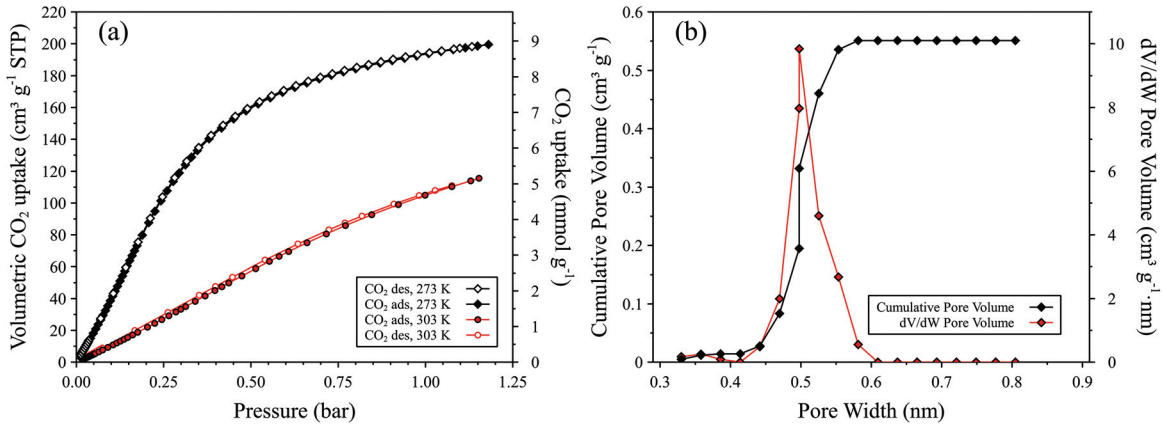

Fig. 4 (a) Manometric carbon dioxide gas sorption isotherms (legend inset) and (b) pore size distribution (PSD, red) and cumulative pore volume plot (black) for MFM-300(Al)-MW. Data calculated from the adsorption branch of the CO_2 isotherm at 273 K using the NLDFT model for carbon slit pores.[26–28]

Fig. 4a) show very high uptake capacities, with a maximum value of 8.8 mmol g^{-1} at 273 K and 1.0 bar and 4.7 mmol g^{-1} at 303 K and 1.0 bar. Analysis of the adsorption branch of the CO_2 isotherm at 273 K gave a BET surface area of 1272 ± 25 m^2 g^{-1}. The non-local density functional theory (NLDFT) model for carbon slit pores[26–28] gave a pore size distribution centred at 0.5 nm whereby the total pore volume is reached at 0.6 nm, indicative of a solely microporous material,[26] and a cumulative pore volume of 0.58 cm^3 g^{-1} (Fig. 4b). These results differ from the CO_2 sorption properties of MFM-300(Al)-CH whereby a maximum uptake of 7.0 mmol g^{-1} at 273 K and 1.0 bar and cumulative pore volume of 0.38 cm^3 g^{-1} were reported.[12] MFM-300(Al)-MW shows negligible N_2 sorption at 298 K up to 1 bar (see Fig. 5a), however at 77 K a Type I isotherm, with some Type IV character, is observed (Fig. 5b). From these data, an N_2 uptake of 135 cm^3 g^{-1} at *ca.* 0.5 bar and BET surface area of 515 ± 1 m^2 g^{-1} were calculated (Fig. 5b). These results are significantly different compared to MFM-300(Al)-CH which does not adsorb dinitrogen.[10–12] The lack of N_2 porosity demonstrated by MFM-300(Al)-CH is not expected for an open porous structure and was ascribed by Yang *et al.* to restricted diffusion at low temperatures as a result of the narrow pore channels.[12] Further work is ongoing to investigate the difference in porosity between microwave and conventionally heated MFM-300(Al) materials.

We also determined the SO_2 and NO_2 sorption properties of MFM-300(Al)-MW which, like MFM-300(Al)-CH, exhibits exceptional uptake capacities for these environmentally detrimental gases. The high uptake of SO_2 and NO_2 exhibited by MFM-300(Al) are a result of multiple formal interactions between the bridging μ_2-OH functionality of the aluminium secondary building unit with guest molecules, resulting in an efficient packing of SO_2 and NO_2 within the pore.[12,15,16] SO_2 adsorption isotherms at 283 K, 298 K and 303 K for MFM-300(Al)-MW collected using 25% SO_2 in N_2 are shown in Fig. 5a and are summarised in Table 1. As can be seen, MFM-300(Al)-

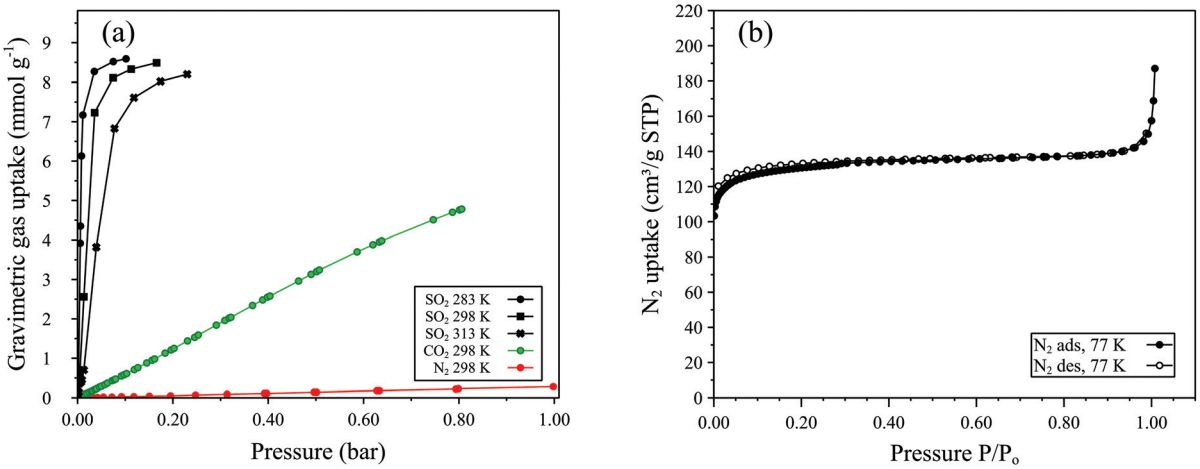

Fig. 5 (a) Gravimetric SO_2 and manometric CO_2, and N_2 gas adsorption isotherms and (b) manometric N_2 gas sorption isotherm at 77 K for MFM-300(Al)-MW. Legends inset. SO_2 data were collected using 25% SO_2 in N_2 as the sorbate.

Table 1 Comparison of SO_2 uptake of selected MOFs

	SO_2 uptake (mmol g^{-1})					
	Pressure (bar)				Temperature	
Material	0.01	0.10	0.17	1.00	(K)	Ref.
MFM-300(Al)-MW	7.2	8.6	—	—	283	This work
	2.6[b]	8.1[c]	8.5	—	298	This work
	0.5	7.6[d]	8.0	—	313	This work
MFM-300(Al)-CH	—	—	—	8.1	273	12
		~4.5[a]	~5[a]	~5[a]	298	16
MFM-300(In)	—	—	—	8.3	298	34
MOF-177	0.3	1.0	1.5[a]	25.7	293	29
NH_2-MIL-125(Ti)	3.0	7.9	~8.6[a]	10.8	293	29
	—	5[a]	~7[a]	9.7[a]	298	35
MIL-160	4.2	5.5	~5.8[a]	10.8	293	29
SIFSIX-1-Cu	3.4	8.7	—	11.0	298	36
SIFSIX-2-Cu-i	4.2	6.0	—	6.9	298	36

[a] Taken from isotherm. [b] At 0.013 bar. [c] At 0.074 bar. [d] At 0.12 bar.

MW exhibits high SO_2 uptakes, 8.49 mmol g^{-1} at 298 K and 0.17 bar partial pressure (P), exceeding the previously reported ~5 mmol g^{-1} at the same temperature and pressure,[16] and 8.1 mmol g^{-1} at 273 K and P = 1.0 bar.[12] As with the previously reported MFM-300(Al)-CH, the SO_2 uptake for MFM-300(Al)-MW (Fig. 5a) show a steep increase at low pressure (<0.01 bar P) followed by a less steep increase up to 0.1 bar P, indicative of a Type I isotherm.[12] At a P of 0.10 bar and 298 K, MFM-300 (Al)-MW exhibits the second highest reported SO_2 uptake capacity compared to other MOFs (Table 1) which is promising for potential applications in SO_2 capture from flue gas where the concentration of SO_2 is typically <500 ppm[29] or for low concentration SO_2 gas detection.[17] NO_2 uptake by MFM-300 (Al)-MW was confirmed by measuring single point adsorption at 273 K, 298 K and 313 K using a mixture of 1% NO_2 in N_2 (see Fig. 6). At a P of 0.01 bar and 298 K, MFM-300(Al)-MW shows an NO_2 uptake of 1.89 mmol g^{-1} which exceeds the reported NO_2 uptake of 1.02 mmol g^{-1} for MFM-300(Al)-CH at the equivalent pressure.[16]

In conclusion, the rapid synthesis of MFM-300(Al) in aqueous conditions using microwave heating has been developed. This route yields MFM-300(Al) on the tens of milligram scale in just 10 minutes with significantly enhanced uptake of polluting dioxides (8.8 *cf.* 7.0 mmol g^{-1} CO_2 at 273 K and 1 bar,[10–12] 8.5 *cf.* ~5 mmol g^{-1} SO_2 at 298 K and 0.17 bar,[12,16] and 1.9 *cf.* 1.0 mmol g^{-1} NO_2 at 298 K and 0.01 bar.[17] Other essential properties of MFM-300(Al) such as surface area (1272 ± 26 m^2 g^{-1}) and temperature of decomposition (>500 °C) are maintained. This is the fastest reported synthesis of MFM-300(Al) to date with a 99.77% reduction in reaction time compared to current solvothermal methods (3 days). The efficient and facile procedure in this work represents a key step towards the development of a sustainable route to MFM-300 (Al), and possibly other MOFs, by reducing the environmental burden (use of aqueous solvent and very short reaction times). This new method also offers favourable conditions (*e.g.* short timescales) for development of a continuous and scalable production route using microwave heating. Industry has identified the need for new sustainable routes to MOFs[30] as a prerequisite for their use in real-world applications addressing major world-wide concerns in environmental air pollution.

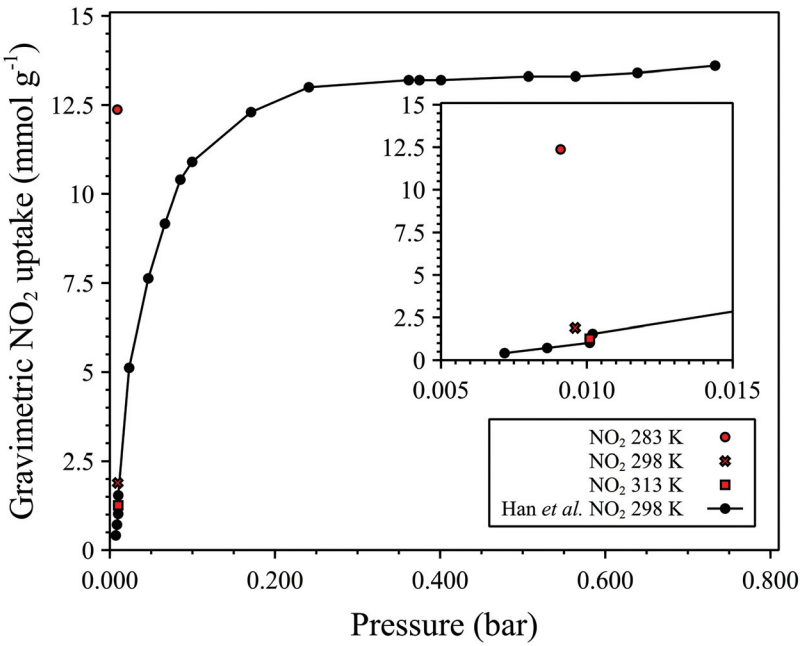

Fig. 6 Single point NO_2 sorption data collected for MFM-300(Al)-MW at 283 K, 298 K, and 313 K corresponding to partial pressures between 0.009 and 0.01 bar using 1% NO_2 in N_2 as the sorbate (in red). NO_2 isotherm at 298 K reported by Han *et al.* (ref. 10) for MFM-300(Al)-CH for comparison in black (sorbate is pure NO_2). Legend inset.

Experimental section

Materials and methods

Synthesis of MFM-300(Al)-MW. Aluminium trichloride hexahydrate (99%) and biphenyl-3,3′,5,5′-tetracarboxylic acid (95%) were obtained from Alfa Aesar and Manchester Organics Limited, respectively, and used as received. Milli-Q plus 18.2 MΩ cm deionized water was used.

$AlCl_3{\cdot}6H_2O$ (250 mg, 1.04 mmol), biphenyl-3,3′,5,5′-tetracarboxylic acid (H_4BPTC, 85 mg, 0.26 mmol) and deionized water (15.0 mL) were added to a 35 mL vial. The vial was sealed and contents stirred to facilitate dissolution of the metal salt. The vial was then placed in to a CEM Discover microwave cavity and heated to 210 °C for 10 minutes (300 W, maximum forward power) under autogenous pressure and with stirring. After the reaction time had elapsed the vial was cooled in the microwave cavity with air and the resultant suspension was centrifuged (4200 revolutions per minute, 20 minutes) and washed with distilled water (*ca.* 50 mL). The centrifugation and wash step was repeated twice and the supernatant decanted. The white powder product was then dried in an oven at 50 °C for 18 hours. After this time the sample was allowed to rehydrate in the fumehood under ambient atmospheric conditions for 8 hours. Yield (89 mg, 83.5%; for the dehydrated MOF, *i.e.* $[Al_2(OH)_2(C_{16}O_8H_6)]$, calculated based on the linker and TGA analyses). Further details on synthetic development can be found in the ESI.†

Characterisation

Powder X-ray diffraction. Diffraction patterns were collected using a PANalytical MPD diffractometer equipped with a PIXcel DKIW179H1 detector and a conventional sealed tube Cu X-ray source (operating at 40 kV and 40 mA), equipped with an α1 monochromator. Scans were conducted between 2° and 70° 2θ and data were analysed using TOPAS Academic[31] and are plotted using Veusz.[32]

Thermogravimetric analyses. Thermogravimetric analyses were carried out using either a TA instruments TGA 550 or Q5000IR analyser. Samples were heated at a rate of 2 K min^{-1} under a nitrogen atmosphere to a maximum of 800 °C. Data plotted using Veusz.[32]

Scanning electron microscopy. High-resolution SEM images of MFM-300(Al) were collected using a JEOL 7100F FEG-scanning electron microscope. Samples were prepared on machined aluminium stubs with carbon adhesive tabs. The samples were coated with a 10 nm layer of iridium using a Quorum QISOT ES coater. Imaging was conducted at a working distance of 10 mm with an electron gun accelerating potential of 15 kV. Frame captures of the sample morphologies were obtained using Jeol PC-SEM software. Average particle size and standard deviation were determined by measuring the length and diameter of a total of 50 particles using ScionImage software.[33]

Gas sorption. Manometric CO_2 sorption isotherms were recorded at 273 K and 303 K up to 1.2 bar using either a Micromeritics 3Flex or a Micromeritics ASAP 2420 adsorption analyser. In a typical measurement between 100 and 150 data points were collected. Surface areas were calculated in the relative pressure (P/P_0) range from 0.01 to 0.015 which corresponds to a pressure of <0.5 bar; in this region all of the micropores are filled. PSD and cumulative pore volume were calculated from the adsorption branch of the CO_2 isotherm at 273 K using the NLDFT pore model for carbon slit pore geometry.[26–28] Manometric N_2 sorption was recorded at 77 K up to 1.0 bar using a Micromeritics ASAP 2420 adsorption analyser; *ca.* 100 data points were collected. Samples were degassed at 120 °C for 15 hours under vacuum (10^{-5} bar) before analysis. Data were analysed using Micromeritics MicroActive software (V5) and plotted using Veusz.[32]

Gravimetric SO_2 and NO_2 adsorption isotherms were recorded using a magnetic suspension balance working in the dynamic flow mode at ambient pressure. Therefore, an inert gas flow of dry nitrogen was used to balance the SO_2 concentration between SO_2 partial pressure 0.002–0.2. SO_2 data were collected at temperatures of 283 K, 298 K, and 313 K and partial pressures up to 0.10, 0.17 and 0.232 bar using 25% SO_2 in N_2 as the sorbate. Single point NO_2 sorption data were collected at 283 K, 298 K, and 313 K corresponding to partial pressures between 0.009 and 0.01 bar using 1% NO_2 in N_2 as the sorbate. Samples were degassed in a nitrogen flow at 120 °C until no further decrease in weight was observed.

Manometric CO_2 and N_2 sorption isotherms were recorded using a stainless-steel version of the BELSORP-max sorption analyser at 298 K and up to 0.81 and 1.0 bar, respectively. In a typical measurement between 30 and 60 data points were collected. Samples were degassed at 120 °C for 15 hours under vacuum (10^{-7} bar) before analysis. Data were plotted using Veusz.[32]

Conflicts of interest

There are no conflicts of interest to declare.

Acknowledgements

SEM analyses in this work were supported by the Engineering and Physical Sciences Research Council (EPSRC) [under grant EP/L022494/1] and the University of Nottingham. Andrea Laybourn gratefully acknowledges the University of Nottingham for the award of a Nottingham Research Fellowship.

References

1 M. Kampa and E. Castanas, Human health effects of air pollution, *Environ. Pollut.*, 2008, **151**, 362–367.
2 J. N. Galloway, Acid deposition: Perspectives in time and space, *Water, Air, Soil Pollut.*, 1995, **85**, 15–24.
3 D. W. Keith, Why Capture CO_2 from the Atmosphere?, *Science*, 2009, **325**, 1654–1655.

4 P. M. Edwards, S. S. Brown, J. M. Roberts, R. Ahmadov, R. M. Banta, J. A. deGouw, W. P. Dubé, R. A. Field, J. H. Flynn, J. B. Gilman, M. Graus, D. Helmig, A. Koss, A. O. Langford, B. L. Lefer, B. M. Lerner, R. Li, S.-M. Li, S. A. McKeen, S. M. Murphy, D. D. Parrish, C. J. Senff, J. Soltis, J. Stutz, C. Sweeney, C. R. Thompson, M. K. Trainer, C. Tsai, P. R. Veres, R. A. Washenfelder, C. Warneke, R. J. Wild, C. J. Young, B. Yuan and R. Zamora, High winter ozone pollution from carbonyl photolysis in an oil and gas basin, *Nature*, 2014, **514**, 351–354.

5 J. Lelieveld, T. M. Butler, J. N. Crowley, T. J. Dillon, H. Fischer, L. Ganzeveld, H. Harder, M. G. Lawrence, M. Martinez, D. Taraborrelli and J. Williams, Atmospheric oxidation capacity sustained by a tropical forest, *Nature*, 2008, **452**, 737–740.

6 Z. Chen, J.-N. Wang, G.-X. Ma and Y.-S. Zhang, China tackles the health effects of air pollution, *Lancet*, 2013, **382**, 1959–1960.

7 V. L. Feigin, G. A. Roth, M. Naghavi, P. Parmar, R. Krishnamurthi, S. Chugh, G. A. Mensah, B. Norrving, I. Shiue, M. Ng, K. Estep, C. J. L. Cercy, M. H. Murray and I. Forouzanfar, Global Burden of Diseases, Risk Factors Study 2013, Stroke Experts Writing Group. Global burden of stroke and risk factors in 188 countries, during 1990–2013: a systematic analysis for the Global Burden of Disease Study 2013, *Lancet Neurol.*, 2016, **15**, 913–924.

8 E. Barea, C. Montoro and J. A. R. Navarro, Toxic gas removal – metal–organic frameworks for the capture and degradation of toxic gases and vapours, *Chem. Soc. Rev.*, 2014, **43**, 5419–5430.

9 K. Sumida, D. L. Rogow, J. A. Mason, T. M. McDonald, E. D. Bloch, Z. R. Herm, T.-H. Bae and J. R. Long, Carbon Dioxide Capture in Metal–Organic Frameworks, *Chem. Rev.*, 2012, **112**, 724–781.

10 X. Han, H. G. W. Godfrey, L. Briggs, A. J. Davies, Y. Cheng, L. L. Daemen, A. M. Sheveleva, F. Tuna, E. J. L. McInnes, J. Sun, C. Drathen, M. W. George, A. J. Ramirez-Cuesta, K. M. Thomas, S. Yang and M. Schröder, Reversible adsorption of nitrogen dioxide within a robust porous metal–organic framework, *Nat. Mater.*, 2018, **17**, 691–696.

11 S. Yang, A. J. Ramirez-Cuesta, R. Newby, V. Garcia-Sakai, P. Manuel, S. K. Callear, S. I. Campbell, C. C. Tang and M. Schröder, Supramolecular binding and separation of hydrocarbons within a functionalized porous metal–organic framework, *Nat. Chem.*, 2015, **7**, 121–129.

12 S. Yang, J. Sun, A. J. Ramirez-Cuesta, S. K. Callear, W. I. F. David, D. P. Anderson, R. Newby, A. J. Blake, J. E. Parker, C. C. Tang and M. Schröder, Selectivity and direct visualization of carbon dioxide and sulfur dioxide in a decorated porous host, *Nat. Chem.*, 2012, **4**, 887–894.

13 C. G. Morris, N. M. Jacques, H. G. W. Godfrey, T. Mitra, D. Fritsch, Z. Lu, C. A. Murray, J. Potter, T. M. Cobb, F. Yuan, C. C. Tang, S. Yang and M. Schröder, Stepwise observation and quantification and mixed matrix membrane separation of CO_2 within a hydroxy-decorated porous host, *Chem. Sci.*, 2017, **8**, 3239–3248.

14 C. P. Krap, R. Newby, A. Dhakshinamoorthy, H. García, I. Cebula, T. L. Easun, M. Savage, J. E. Eyley, S. Gao, A. J. Blake, W. Lewis, P. H. Beton, M. R. Warren, D. R. Allan, M. D. Frogley, C. C. Tang, G. Cinque, S. Yang and M. Schröder, Enhancement of CO_2 Adsorption and Catalytic Properties by Fe-Doping of $[Ga_2(OH)_2(L)]$ (H_4L = Biphenyl-3,3′,5,5′-tetracarboxylic Acid), MFM-300(Ga_2), *Inorg. Chem.*, 2016, **55**, 1076–1088.

15 H. G. W. Godfrey, I. da Silva, L. Briggs, J. H. Carter, C. G. Morris, M. Savage, T. L. Easun, P. Manuel, C. A. Murray, C. C. Tang, M. D. Frogley, G. Cinque, S. Yang and M. Schröder, Ammonia Storage by Reversible Host–Guest Site Exchange in a Robust Metal–Organic Framework, *Angew. Chem., Int. Ed.*, 2018, **57**, 14778–14781.

16 X. Han, S. Yang and M. Schröder, Porous metal–organic frameworks as emerging sorbents for clean air, *Nat. Rev. Chem.*, 2019, **3**, 108–118.

17 T. Jurado-Vázquez, E. Sánchez-González, A. E. Campos-Reales-Pineda, A. Islas-Jácome, E. Lima, E. González-Zamora and I. A. Ibarra, MFM-300: From air pollution remediation to toxic gas detection, *Polyhedron*, 2019, **157**, 495–504.

18 V. Chernikova, O. Yassine, O. Shekhah, M. Eddaoudi and K. N. Salama, Highly sensitive and selective SO_2 MOF sensor: the integration of MFM-300 MOF as a sensitive layer on a capacitive interdigitated electrode, *J. Mater. Chem. A*, 2018, **6**, 5550–5554.

19 U. Mueller, M. Schubert, F. Teich, H. Puetter, K. Schierle-Arndt and J. Pastre, Metal-organic frameworks-prospective industrial applications, *J. Mater. Chem.*, 2006, **16**, 626–636.

20 N. Stock and S. Biswas, Synthesis of Metal-Organic Frameworks (MOFs): Routes to Various MOF Topologies, Morphologies, and Composites, *Chem. Rev.*, 2012, **112**, 933–969.

21 I. Thomas-Hillman, A. Laybourn, C. Dodds and S. W. Kingman, Realising the environmental benefits of metal-organic frameworks: recent advances in microwave synthesis, *J. Mater. Chem. A*, 2018, **6**, 11564–11581.

22 M. Rubio-Martinez, C. Avci-Camur, A. W. Thornton, I. Imaz, D. Maspoch and M. R. Hill, New synthetic routes towards MOF production at scale, *Chem. Soc. Rev.*, 2017, **46**, 3453–3480.

23 A. Laybourn, J. Katrib, R. S. Ferrari-John, C. G. Morris, S. Yang, O. Udoudo, T. L. Easun, C. Dodds, N. R. Champness, S. W. Kingman and M. Schroder, Metal-organic frameworks in seconds *via* selective microwave heating, *J. Mater. Chem. A*, 2017, **5**, 7333–7338.

24 A. Le Bail, H. Duroy and J. L. Fourquet, *Ab initio* structure determination of $LiSbWO_6$ by X-ray powder diffraction, *Mater. Res. Bull.*, 1988, **23**, 447–452.

25 X. Bokhimi, J. A. Toledo-Antonio, M. L. Guzmán-Castillo, B. Mar-Mar, F. Hernández-Beltrán and J. Navarrete, Dependence of Boehmite Thermal Evolution on Its Atom Bond Lengths and Crystallite Size, *J. Solid State Chem.*, 2001, **161**, 319–326.

26 K. S. W. Sing, Reporting physisorption data for gas/solid systems with special reference to the determination of surface area and porosity (Recommendations 1984), *Pure Appl. Chem.*, 1985, **57**, 603.
27 J. J. Manyà, B. González, M. Azuarab and G. Arner, Ultramicroporous adsorbents prepared from vine shoots-derived biochar with high CO_2 uptake and CO_2/N_2 selectivity, *Chem. Eng. J.*, 2018, **345**, 631–639.
28 A. C. Dassanayake and M. Jaroniec, Activated polypyrrole-derived carbon spheres for superior CO_2 uptake at ambient conditions, *Colloids Surf., A*, 2018, **549**, 145–154.
29 P. Brandt, A. Nuhnen, M. Lange, J. Möllmer, O. Weingart and C. Janiak, Metal–Organic Frameworks with Potential Application for SO_2 Separation and Flue Gas Desulfurization, *ACS Appl. Mater. Interfaces*, 2019, **11**(19), 17350–17358.
30 P. A. Julien, C. Mottillo and T. Friščić, Metal–organic frameworks meet scalable and sustainable synthesis, *Green Chem.*, 2017, **19**, 2729–2747.
31 A. A. Coelho, TOPAS and TOPAS-Academic: an optimization program integrating computer algebra and crystallographic objects written in C++, *J. Appl. Crystallogr.*, 2018, **51**, 210–218.
32 https://veusz.github.io/2019.
33 https://scion-image.software.informer.com/2019.
34 M. Savage, Y. Cheng, T. L. Easun, J. E. Eyley, S. P. Argent, M. R. Warren, W. Lewis, C. Murray, C. C. Tang, M. D. Frogley, G. Cinque, J. Sun, S. Rudić, R. T. Murden, M. J. Benham, A. N. Fitch, A. J. Blake, A. J. Ramirez-Cuesta, S. Yang and M. Schröder, Selective Adsorption of Sulfur Dioxide in a Robust Metal–Organic Framework Material, *Adv. Mater.*, 2016, **28**, 8705–8711.
35 W. P. Mounfield, C. Han, S. H. Pang, U. Tumuluri, Y. Jiao, S. Bhattacharyya, M. R. Dutzer, S. Nair, Z. Wu, R. P. Lively, D. S. Sholl and K. S. Walton, Synergistic Effects of Water and SO_2 on Degradation of MIL-125 in the Presence of Acid Gases, *J. Phys. Chem. C*, 2016, **120**, 27230–27240.
36 X. Cui, Q. Yang, L. Yang, R. Krishna, Z. Zhang, Z. Bao, H. Wu, Q. Ren, W. Zhou, B. Chen and H. Xing, Ultrahigh and Selective SO_2 Uptake in Inorganic Anion-Pillared Hybrid Porous Materials, *Adv. Mater.*, 2017, **29**, 1606929.